Journal of Hazardous Materials 179 (2010) 332–339

Contents lists available at ScienceDirect

Journal of Hazardous Materials

journal homepage: www.elsevier.com/locate/jhazmat

Adsorption of Pb(II) ions from aqueous solution by native and activated bentonite: Kinetic, equilibrium and thermodynamic study

Ali Rıza Kul[a], Hülya Koyuncu[b,*]

[a] Yuzuncu Yil University, Faculty of Art and Science, Department of Chemistry, 65080 Van, Turkey
[b] Forensic Medicine Foundation, Felek Street No. 45, 06300 Kecioren, Ankara, Turkey

ARTICLE INFO

Article history:
Received 6 November 2009
Received in revised form 27 January 2010
Accepted 3 March 2010
Available online 9 March 2010

Keywords:
Pb(II)
Adsorption
Kinetics
Equilibrium
Thermodynamic

ABSTRACT

In this study, the adsorption kinetics, equilibrium and thermodynamics of Pb(II) ions on native (NB) and acid activated (AAB) bentonites were examined. The specific surface areas, pore size and pore-size distributions of the samples were fully characterized. The adsorption efficiency of Pb(II) onto the NB and AAB was increased with increasing temperature. The kinetics of adsorption of Pb(II) ions was discussed using three kinetic models, the pseudo-first-order, the pseudo-second-order and the intra-particle diffusion model. The experimental data fitted very well the pseudo-second-order kinetic model. The initial sorption rate and the activation energy were also calculated. The activation energy of the sorption was calculated as 16.51 and 13.66 kJ mol^{-1} for NB and AAB, respectively. Experimental results were also analysed by the Langmuir, Freundlich and Dubinin–Redushkevich (D–R) isotherm equations at different temperatures. R_L separation factor for Langmuir and the n value for Freundlich isotherm show that Pb(II) ions are favorably adsorbed by NB and AAB. Thermodynamic quantities such as Gibbs free energy (ΔG), the enthalpy (ΔH) and the entropy change of sorption (ΔS) were determined as about −5.06, 10.29 and 0.017 kJ mol^{-1} K^{-1}, respectively for AAB. It was shown that the sorption processes were an endothermic reactions, controlled by physical mechanisms and spontaneously.

1. Introduction

Among the different heavy metals, lead is one of the common and toxic pollutants released into the natural waters from various industrial activities such as metal plating, oil refining, paint and pigment producing and battery manufacturing [1]. Lead can enter the human body through inhalation, ingestion or skin contact. As a result when the body is exposed to lead, it can act as a cumulative poison. Lead accumulates mainly in bones, brain, kidney and muscles and may cause many serious disorders like anemia, kidney diseases, nervous disorder and sickness even death [2–4]. Lead can replace calcium, which is an essential mineral for strong bones and teeth, while play important role in sympathetic actions of nerve and blood vessel for normal functioning of nervous system. It also acts as an enzyme inhibitor in body, e.g., replaces essential element zinc from heme enzymes. The high level of lead damages cognitive development especially in children [5]. Due to toxic effects of lead ions, the removal of them from waters and wastewaters is important in terms of protection of public health and environment [6].

The conventional methods for heavy metal removal from water and wastewater include oxidation, reduction, precipitation, reverse osmosis, ion exchange, electrolysis and adsorption. Among all the methods adsorption is highly effective and economical [7]. However, the main disadvantage of adsorption treatment is the high price of the adsorbents, which increases the price of wastewater treatment. Thus, adsorbents with low cost and high efficiency for Pb(II) adsorption should be developed. Clay minerals have great potential as inexpensive and efficient adsorbents due to their large quantities, chemical and mechanical stability, high specific surface area, and structural properties. Bentonite is mainly composed of montmorillonite, which is a 2:1-type aluminosilicate. The inner layer is composed of an octahedral sheet situated between two SiO_4 tetrahedral sheets. Substitutions within the lattice structure of trivalent aluminium for quadrivalent silicon in the tetrahedral sheet and of ions of lower valence, particularly magnesium, for trivalent aluminium in the octahedral sheet result in a net negative charge on the clay surfaces. The charge imbalance is offset by exchangeable cations such as H^+, Na^+ or Ca^{2+} on the layer surfaces [8–10]. In aqueous solutions, water molecules are intercalated into the interlamellar space of bentonite, leading to an expansion of the minerals [11]. The chemical nature and pore structure of bentonites generally determine their adsorption ability [12,13]. Treatment of clay minerals with concentrated inorganic acids usually at high temperature is known as acid activation.

* Corresponding author at: Forensic Medicine Foundation, Felek street No:45, 06300 Kecioren, Ankara, Turkey. Tel.: +90 312 3407324; fax: +90 312 3406629.
E-mail address: hkoyuncu@yyu.edu.tr (H. Koyuncu).

0304-3894/$ – see front matter © 2010 Elsevier B.V. All rights reserved.
doi:10.1016/j.jhazmat.2010.03.009

Nomenclature

A	Frequency factor
c	A constant for intra-particle diffusion (mg g^{-1})
C_0	Initial concentration of the adsorbate in the solution (mg L^{-1})
C_e	Equilibrium concentration of the adsorbate in the solution (mg L^{-1})
E	Mean adsorption energy (kJ mol^{-1})
E_a	Activation energy of sorption (kJ mol^{-1})
k_0	Initial sorption rate (mg g^{-1} min^{-1})
k_1	Rate constant for pseudo-first-order reaction (min^{-1})
k_2	Rate constant for pseudo-second-order reaction (g mg^{-1} min^{-1})
k_i	Intra-particle diffusion rate constant (mg g^{-1} min$^{-1/2}$)
k_f	Freundlich isotherm constant
K	Langmuir isotherm constant (L mg^{-1})
K'	Adsorption energy constant (mol^2 kJ^{-2})
m	Amount of bentonite (g)
n	Freundlich isotherm constant
q_0	Maximum concentration retained by the adsorbent (mg g^{-1})
q_e	Amount solute sorbed at equilibrium (mg g^{-1})
q_m	Theoretical monolayer saturation capacity (mol g^{-1})
q_t	Amount solute sorbed at any time (mg g^{-1})
R	Universal gas constant (J mol^{-1} K^{-1})
t	Time (min)
T	Absolute temperature (K)

Acid treatments of clay minerals are an important control over mineral weathering and genesis [14]. Such treatments can often replace exchangeable cations with H^+ ions and release Al and other cations out of both tetrahedral and octahedral sites, but leaving the SiO_4 groups largely intact. The ion exchange capacity of clay minerals is attributed to structural defects, broken bonds and structural hydroxyl transfers [15]. Also, acid treatment of bentonite has been shown to create enhanced mesoporosity with important textural and structural changes [16,17]. The objective of this study is to investigate comparative adsorption characteristics for removal of Pb(II) from aqueous solution by the use of native bentonite (NB) and acid activated bentonite (AAB). The effect of several parameters such as contact time, Pb(II) concentration and temperature were studied. The adsorption mechanism of Pb(II) ions onto NB and AAB were evaluated in terms of kinetics, equilibrium and thermodynamics. The data obtained from the batch sorption experiments were fitted to pseudo-first-order, pseudo-second-order and intra-particle diffusion models. The Langmuir, Freundlich and Dubinin–Radushkevich (D–R) isotherm models were used to describe equilibrium data.

2. Materials and methods

2.1. Materials

The bentonite sample used in this study was obtained from Kütahya region in Turkey. The chemical constituent of the bentonite was analysed by XRF and given in Table 1. A stock solution of Pb(II) was prepared by dissolving required amount of $Pb(NO_3)_2$ (Merck) in double distilled water at room temperature. Other agents used, such as HCl and silver acetate were all of analytical grade.

2.1.1. Preparation and characterization of samples

In order to increase the surface area and provide physico-chemical changes in the structure of bentonite, acid activation test was performed. The acid treatment was carried out using a Pyrex glass reactor with reflux condenser. The reactor was placed onto Chiltern Hotplate Magnetic Stirrer HS 31. 50 g raw bentonite was slowly added to 250 mL 5N HCl solution, stirred and maintained at boiling temperature (approximately 378 K) during 3 h. After treatment, the reaction products were filtered and 15 times washed with distilled water to remove traces of acid. After each washing Cl^- ions were detected with silver acetate solution and then the sample was centrifuged with MSE MISTRAL 2000 at 4500 rpm for 5 min. The final sample was centrifuged and kept at 333 K in an oven (Philip Harris Ltd.) to remove some of the moisture for 48 h. The sample was milled passing 235 mesh sieve (61.75 μm) to eliminate the formation of lumps produced during drying and saved in a desiccator [14–16]. Specific surface areas (BET) and pore-size distributions of the raw and activated bentonite samples were determined using a Quantachrome NOVA 2200 series volumetric gas adsorption instrument. The determinations were based on measurements of the corresponding nitrogen adsorption isotherms at 77 K. Before measurements, moisture and gases such as nitrogen and oxygen that were adsorbed on the solid surface or held in the open pores were removed under reduced pressure at 423 K for 5 h. Cation exchange capacities (CEC) of raw (NB) and activated bentonites (AAB) were determined via methylene blue test (ANSI/ASTM C837-76).

2.2. Methods

Equilibrium and kinetic studies were performed with NB and AAB. Adsorption studies were performed by the batch technique at different temperatures (303 K, 318 K and 328 K). The batch mode adsorption was selected due to its simplicity and reliability. For that purpose, 10 mL of Pb(II) solution in the concentration range of 5–25 mg L^{-1} was transferred into a polyethylene test tube. Then 0.1 g of the bentonite sample was added to the solution and the mixture was shaken at 300 rpm using a thermostatic shaker for each corresponding time intervals. The suspension was centrifuged (Philip Harris Ltd.) at 5000 rpm for 10 min. The supernatant was filtered and the filtrate was analysed for Pb level by flame atomic absorption spectrophotometer (FAAS). The reproducibility during concentration measurements was ensured by repeating the experiments two times under identical conditions and calculating the average values. Standard deviations of experiments were found to be within ±5.0%.

The adsorption capacity of adsorbent was calculated through the following equation:

$$q_e = \frac{(C_0 - C_e)V}{m} \quad (1)$$

where q_e is the adsorption capacity of Pb(II) on adsorbent (mg g^{-1}), C_0 is the initial concentration of Pb(II) (mg L^{-1}), C_e is the equilibrium Pb(II) concentration in solution (mg L^{-1}), m is the mass of adsorbent used (g) and V is the volume of Pb(II) solution (L).

3. Results and discussion

3.1. Characterization of the samples

Nitrogen adsorption isotherms of NB and AAB samples are shown in Fig. 1. The specific surface areas of the samples were calculated from nitrogen adsorption isotherms by the BET method mainly for comparative purposes. AAB markedly affected N_2 adsorption characteristics of the bentonite. However, the general shape of the isotherm stayed at the same, after the activation relatively increased the nitrogen uptake as seen in Fig. 1.

Table 1
The chemical composition of Kütahya bentonite.

	SiO_2	Al_2O_3	Fe_2O_3	TiO_2	CaO	MgO	Na_2O	K_2O	LoI[a]	Others
g/100 g	71.600	13.150	0.660	0.070	2.230	2.790	0.260	0.360	8.450	0.430

[a] Loss of ignition at 1025 °C.

The BET surface areas of the samples are also determined. The acid activation causes formation of smaller pores in solid particles resulting higher surface area (109.80 m^2/g) relative to than NB (71.95 m^2/g). For a textural characterization of any porous solid, the concept of surface area does not give a visual picture of it. Pore size and pore-size distributions are necessary if the material is to be fully characterized. The pore-size distribution in the mesopore region was obtained by applying the method of BJH [18] to the desorption branch of the isotherms of nitrogen at 77 K, assuming the pores to be cylindrical in shape. Fig. 2 compares the change of pore-size distribution for the NB and AAB samples. As seen from the figure, the samples have almost mesopores of which diameters are between 20 and 500 Å. The NB and AAB samples exhibited maxima in differential pore volumes at about 39.46 and 34.50 Å in pore diameter respectively. The cation exchange capacities (CEC) of the NB and AAB were found as 65 and 97 mequiv./100 g, respectively.

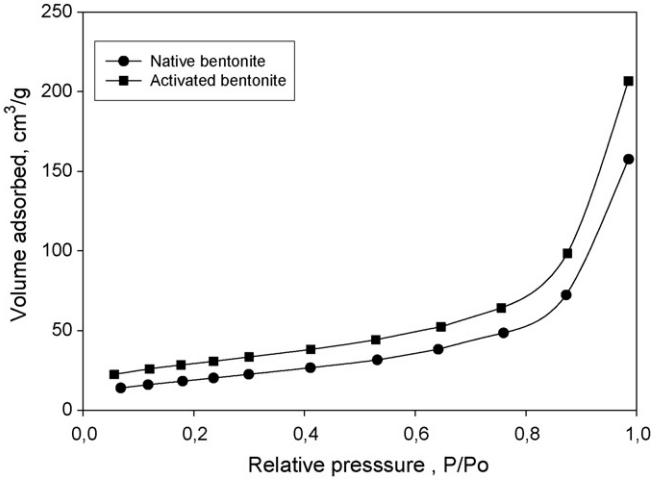

Fig. 1. Adsorption isotherms of nitrogen at 77 K of the native and activated bentonite samples.

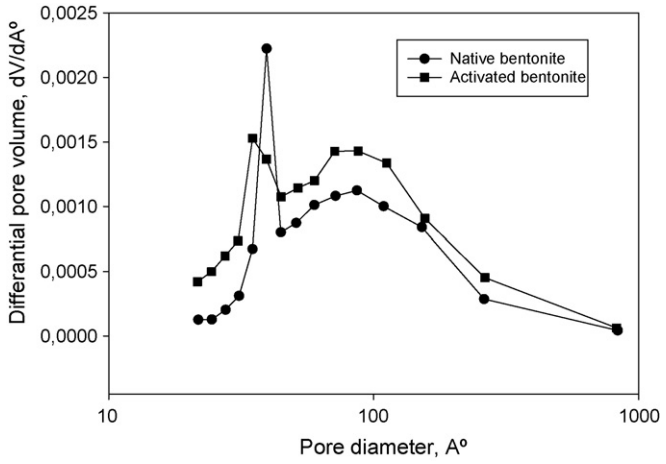

Fig. 2. Pore-size distributions for the native and activated bentonite samples.

3.2. The adsorption efficiency

The results showed that 100 min was enough to reach the dynamic equilibrium between fluid phase and solid phase in all studied solution concentration and temperatures. The adsorption efficiency of Pb(II) ions was calculated by the difference of initial and final concentration using the equation expressed as follows:

$$\text{Ads-Eff } (\%) = \left[\frac{C_0 - C_e}{C_0}\right] \times 100 \quad (2)$$

The adsorption efficiency increases with increasing temperature. The effect of temperature is fairly common and increasing the temperature increase the mobility of the solute. Also, it was explained that the endothermic adsorption enthalpy. Similar results have been reported by [2,17,19]. Adsorption efficiency for AAB reached at about 78% while it was at about 50.4% for NB at 328 K (Fig. 3). It was found that the adsorption efficiency with the AAB was greater than NB in all studied solution concentration and temperatures. It was expected, because the acid activation causes formation of smaller pores in solid particles resulting higher surface area relative to NB. Bhattacharyya and Sen Gupta [15] noted that acid activation increased the adsorbent capacity to a good extent.

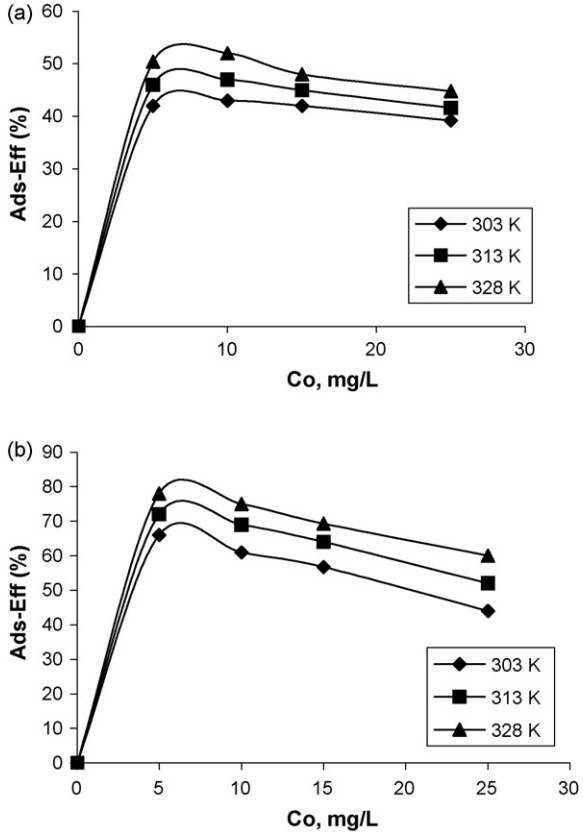

Fig. 3. The adsorption efficiency of Pb(II) onto the native (a) and activated bentonites (b) at various temperatures (equilibrium time 100 min).

Table 2
Comparison of the pseudo-first-order, pseudo-second-order and intra-particle diffusion models for Pb(II) on the native (NB) and activated (AAB) bentonites (303 K and 5 mg L^{-1}).

	$q_{e,exp}$ (mg g^{-1})	$q_{e,cal}$ (mg g^{-1})	k_1 (min^{-1})	R^2	SSE (%)
Pseudo-first-order kinetic model					
NB	0.201	0.119	0.055	0.898	0.079
AAB	0.330	0.228	0.028	0.969	0.104

	$q_{e,exp}$ (mg g^{-1})	$q_{e,cal}$ (mg g^{-1})	Deviation (%)	k_2 (g mg^{-1} min^{-1})	k_0 (g mg^{-1} min^{-1})	R^2	SSE (%)
Pseudo-second-order kinetic model							
NB	0.201	0.214	6.5	0.803	0.037	0.994	0.027
AAB	0.330	0.369	11.6	0.175	0.024	0.995	0.021

	$q_{e,exp}$ (mg g^{-1})	$q_{e,cal}$ (mg g^{-1})	k_i (mg g^{-1} $min^{-1/2}$)	C (mg g^{-1})	R^2	SSE (%)
Intra-particle diffusion model						
NB	0.201	0.192	0.017	0.056	0.672	0.038
AAB	0.330	0.262	0.027	0.071	0.918	0.026

3.3. Kinetic studies

Kinetic models can be helpful to understand the mechanism of metal adsorption and evaluate performance of the adsorbents for metal removal. A number of kinetic models have been developed to describe the kinetics of heavy metal removal: (a) a pseudo-first-order kinetic model of Lagergren [20,21] based on solid capacity, (b) a pseudo-second-order kinetic model of Ho [20,22] based on solid phase sorption, and (c) intra-particle diffusion model of Weber and Morris [22,23]. In this study, batch sorption kinetics of Pb(II) ions with the bentonites have been studied in terms of pseudo-first-order kinetic, pseudo-second-order kinetic and intra-particle diffusion models. First, the kinetics of adsorption was analysed by the pseudo-first-order equation given by Lagergren [21] as,

$$\ln(q_e - q_t) = \ln\ q_e - k_1 t \quad (3)$$

where q_e and q_t are the amounts of solute adsorbed (mg g^{-1}) at equilibrium and at time t (min), respectively, and k_1 (min^{-1}) is the rate constant adsorption. Values of k_1 at 303–328 K were calculated from the plots of $\ln(q_e - q_t)$ versus t (figures not shown) for initial solutions with different concentration of Pb(II). The R^2 values obtained were lower than that of the pseudo-second-order kinetic model and the experimental q_e values did not agree with the calculated values obtained from the linear plots (Table 2). This indicates that the adsorption of Pb(II) NB and AAB does not follow pseudo-first-order kinetics. The similar results were found for the adsorption of Pb(II) ions on various adsorbents by several authors [24,25].

Experimental data were also applied to the pseudo-second-order kinetic model [22] which is given in the following form:

$$\frac{t}{q_t} = \frac{1}{k_2 q_e^2} + \frac{t}{q_e} \quad (4)$$

where k_2 is the rate constant for pseudo-second-order reaction (g mg^{-1} min^{-1}), q_e and q_t are the amounts of solute sorbed at equilibrium and any time (mg g^{-1}), respectively. The straight line plots of t/q_t versus t are used to obtain the constants for pseudo-second-order reaction. Herein, the initial sorption rate is

$$k_0 = k_2 q_e^2 \quad (5)$$

Fig. 4 illustrates pseudo-second-order sorption kinetics of adsorption of Pb(II) onto NB and AAB at various temperatures. The values of correlation factor R^2, obtained from the plots of pseudo-second-order kinetics given in Fig. 4 are greater ($R^2 > 0.99$) than that of the pseudo-first-order and intra-particle diffusion models for all studied initial Pb(II) concentration and temperatures (Table 2). It also showed a good agreement between the experimental and the calculated q_e values (deviations +2.28 to +12.40%, Table 2). The small deviation might be due to the uncertainty inherent in obtaining the experimental q_e values. These results showed that the adsorption of Pb(II) ions onto NB and AAB follows well the pseudo-second-order kinetics. The similar results were reported for the adsorption of Pb(II) on different adsorbents [24,26]. The rate constants k_2, were found as 0.803 and 0.175 g mg^{-1} min^{-1} for NB and AAB at 303 K and 5 mg L^{-1} initial solution concentration (Table 2). Kenedy Oubagaranadin and Murthy [27] reported that the rate of adsorption of Pb(II) on montmorillonite-illite type clay (MIC) followed second order rate mechanism, with decreasing rate constant values of 0.1097, 0.0571 and 0.0022 g mg^{-1} min^{-1} as the initial Pb(II) concentration was increased in the order of 100, 150 and 200 ppm, respectively. Hefne et al. [28] reported that the rate of adsorption of Pb(II) onto natural and treated bentonite followed pseudo-second-order kinetics and rate constant value was determined to be 0.68 g mg^{-1} min^{-1} for natural bentonite.

The metal ions transport from the solution phase to the surface of the clay particles occurs in several steps. The overall adsorption process may be controlled either by one or more steps (e.g., film or external diffusion, pore diffusion, surface diffusion and adsorption on the pore surface) or a combination of more than one step. Besides

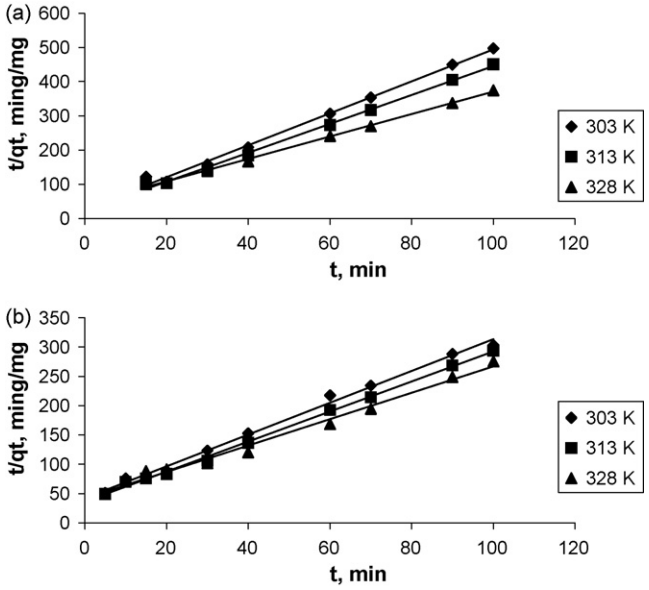

Fig. 4. Effect of temperature on pseudo-second-order kinetics of Pb(II) onto the native bentonite (a) and activated bentonite (b) (5 mg L^{-1} initial solution concentration).

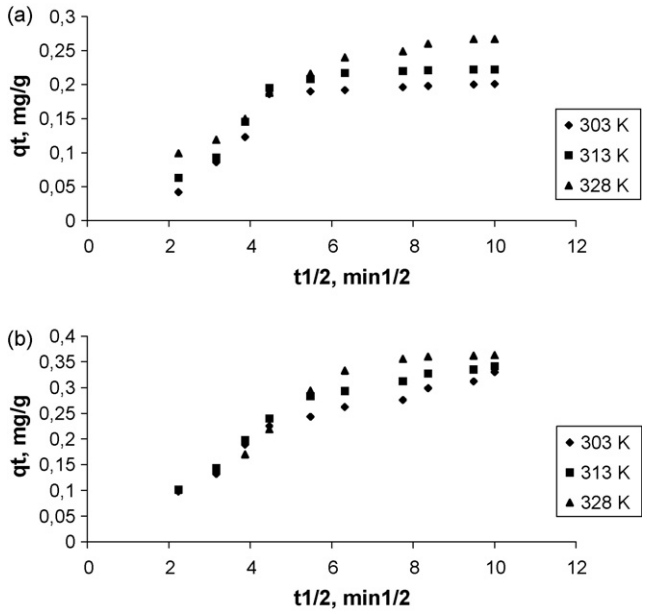

Fig. 5. Effect of temperature on intra-particle diffusion kinetics of Pb(II) onto the native bentonite (a) and activated bentonite (b) (5 mg L^{-1} initial solution concentration).

adsorption at the outer surface of the adsorbent, there is also a possibility of intra-particle diffusion of the metal ion from the bulk of the outer surface into the pores of the adsorbent material, which is usually a slow process. The possibility of intra-particle diffusion studied using the intra-particle diffusion model [2,29,30]:

$$q_t = k_i t^{1/2} + c \quad (6)$$

where k_i is the intra-particle diffusion rate constant (mg g^{-1} $min^{-1/2}$) and c is the intercept. In this model, due to the porous nature of adsorbent, pore diffusion is expended to be surface sorption. According to this model, plotting a graphic of q_t versus $t^{1/2}$, if a straight line is obtained passing through the origin, it can be assumed that the mechanism involves the diffusion of the species and the slope of the linear curve is the rate constant of intra-particle transport (k_i). In the present study, any plot did not passed through the origin and this deviation from the origin might be due to the difference in the mass transfer rate in the initial and final stages of adsorption. The plots present multilinearity, indicating that three steps take place. As can be seen in Fig. 5 (q_t versus $t^{1/2}$) the first, sharper portion may be considered as an external surface adsorption or faster adsorption stage. The second portion describes the gradual adsorption stage, where intra-particle diffusion is rate-controlled. The third portion is attributed to the final equilibrium stage, where intra-particle diffusion starts to slow down due to the extremely low adsorbate concentrations in the solution. In the intermediate stage where the adsorption is gradual, the process may be controlled by intra-particle diffusion. The rate of uptake might be limited by the size of the adsorbate molecule, the concentration of the adsorbate and its affinity to the adsorbent, the diffusion coefficient of the adsorbate in the bulk phase, the pore-size distribution of the adsorbent, and the degree of mixing [31]. The values of R^2, obtained from the plots of intra-particle diffusion kinetics are lower than that of the pseudo-second-order model (Table 2) but this model indicates that the adsorption of Pb(II) onto the NB and AAB may be followed by an intra-particle diffusion model up to 15 min. This indicates that although intra-particle diffusion was involved in the adsorption process, it was not the only rate-controlling step. Kenedy Oubagaranadin and Murthy [27] reported that the adsorption process of Pb(II) on montmorillonite-illite type clay (MIC) was controlled by both intra-particle diffusion and film diffusion.

3.4. Validity of kinetic models

The adsorption kinetics of Pb(II) onto NB and AAB was verified at different initial Pb(II) concentration. The validity of each model determined by sum of squared errors (SSE, %) given by,

$$\mathrm{SSE} = \left[\frac{\sum (q_{e,exp} - q_{e,cal})^2}{N}\right]^{1/2} \quad (7)$$

where N is the number of data points. The lower value of SSE indicates the better a fit is. Table 2 lists the SSE values obtained for the three kinetic models studied. It was found that the pseudo-second-order kinetic model yielded the lowest SSE values. This agrees with the R^2 values obtained earlier and proves that the adsorption of Pb(II) ions onto NB and AAB can be best described by the pseudo-second-order kinetic model.

As a result, it is clear that the values of correlation coefficients obtained for the linear plots from the pseudo-second-order equation are greater than those obtained for the pseudo-first-order and intra-particle diffusion equation under all conditions studied. Also, the values of SSE obtained for the pseudo-second-order equation are lower than those obtained for the pseudo-first-order and intra-particle diffusion equation under all conditions studied. Therefore, it can be said that kinetics of Pb(II) onto NB and AAB complies best with the pseudo-second-order model due to the higher correlation coefficient as reported by Mathialagan and Viraraghavan [30] and lower SSE values as reported Tan et al. [32], and a good agreement between the experimental and the calculated q_e values (Table 2). Also, the kinetics data derived using the intra-particle diffusion model indicates that intra-particle diffusion rate is one of the rate determining steps. This is also confirmed by the activation energy values shown below.

3.5. Activation energy

Generally, a rise in temperature of a chemical reaction increases the rate of the reaction, and the temperature dependence results in a change in the rate constant. Activation energy of the sorption for Pb(II) onto NB and AAB can be estimated by Arrhenius equation providing the relationship between rate constant and temperature as shown in the following:

$$k = A \exp\left(-\frac{E_a}{RT}\right) \quad (8)$$

where k is the rate constant for sorption (g mg^{-1} min^{-1}), A is the Arrhenius constant which is a temperature independent factor (g mg^{-1} min^{-1}), E_a activation energy (kJ mol^{-1}), R universal gas constant (8.314 J mol^{-1} K^{-1}) and T is the solution temperature in Kelvin (K).

In this study, activation energy of sorption process was calculated using the values of the rate constant from a pseudo-second-order kinetic equation at three different temperatures. The values of E_a and A from the Arrhenius plots (figures not shown) for NB and AAB are 16.51 kJ mol^{-1} and 15.62, and 13.66 kJ mol^{-1} and 2.26, respectively. Hence, the Arrhenius equation for the Pb(II)/native bentonite sorption system can be written as follows:

$$k = 15.62 \exp\left(-\frac{16.51 \times 10^3}{RT}\right) \quad (9)$$

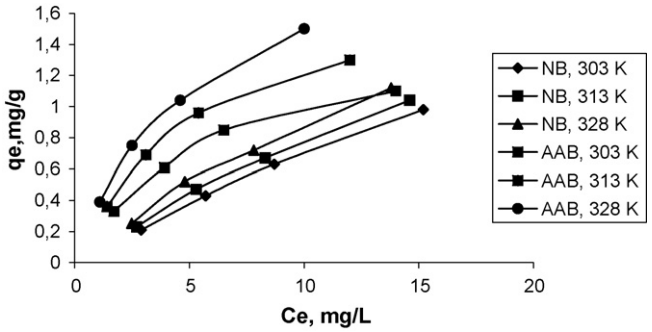

Fig. 6. The adsorption isotherms of Pb(II) on the native and activated bentonites at various temperatures (equilibrium time 100 min).

Eq. (8) can be written for the Pb(II)/activated bentonite sorption system:

$$k = 2.26 \exp\left(-\frac{13.66 \times 10^3}{RT}\right) \quad (10)$$

The values of E_a are low for Pb(II)/native bentonite and Pb(II)/activated bentonite sorption systems. Moreover, the E_a obtained is very low for Pb(II)/activated bentonite sorption system, and thus the sorption process may involve not only an activated process but also a physical sorption.

3.6. Equilibrium studies

The analysis of the isotherms data by fitting them into different isotherm models is an important step to find the suitable model that can be used for design process. It was found that the adsorption equilibrium time of Pb(II) onto NB and AAB was 100 min. Fig. 6 shows the plots of q_e versus of C_e for the adsorption isotherms of Pb(II) on the NB and AAB at various temperatures. These curves are convex upward throughout are designated as favorable type [33]. The experimental data were applied to the Langmuir, Freundlich and D–R, isotherm equations. The constant parameters of the isotherm equations for this adsorption processes were calculated by regression using linear form of isotherm equations. The constant parameters and correlation coefficients (R^2) are summarized in Table 3.

The Langmuir adsorption isotherm [34] has been successfully applied to many real sorption processes. It predicts the maximum monolayer adsorption capacity of the adsorbent and also determines if the adsorption is favorable or not. The linearized Langmuir isotherm is represented by following equation:

$$\frac{C_e}{q_e} = \frac{1}{q_0 K} + \frac{C_e}{q_0} \quad (11)$$

where C_e is the solute concentration at equilibrium (mg L^{-1}), q_e the adsorption capacity in equilibrium (mg g^{-1}), K the Langmuir adsorption constant (L mg^{-1}), and q_0 is the maximum concentration retained by the adsorbent (mg g^{-1}). The Langmuir (C_e/q_e versus C_e) plots of Pb(II) were found to be linear the whole concentration range studied and the correlation coefficients were extremely high. The maximum adsorption capacities were determined as 6.49 mg g^{-1} for Pb(II)/NB and 2.32 mg g^{-1} for Pb(II)/AAB systems (at 328 K). Mishra and Patel [35] reported that the Langmuir adsorption capacities for Pb(II) onto bentonite, kaolin and active carbon were found as 7.56, 4.50 and 6.68 mg g^{-1}, respectively. Han et al. [36] reported that the Langmuir adsorption capacity for Pb(II) on manganese oxide coated sand was found to be 1.34 mg g^{-1}. Eren [19] reported that the adsorption capacities for Pb(II) on raw, iron- and magnesium-coated bentonite were obtained as 16.70, 22.20 and 31.86 mg g^{-1}, respectively. In another study, Kenedy Oubagaranadin and Murthy [27] reported that the maximum monolayer adsorption capacity of Pb(II) on montmorillonite-illite type clay (MIC) was determined to be 52 mg g^{-1}. To determine if adsorption process is favorable or unfavorable, for the Langmuir type adsorption process, isotherm can be classified by a term R_L, a dimensionless constant separation factor, which is defined as below [37]:

$$R_L = \frac{1}{1 + KC_0} \quad (12)$$

The R_L values are found in the range of 0.92–0.98 and 0.51–0.59 for Pb(II) onto NB and AAB at 303–328 K, showing favorable adsorption and a relatively high metal uptake by the adsorbent is achievable at low concentrations in the solution [27,38].

The Freundlich adsorption isotherm model is based on multilayer adsorption. In this model, the mechanism and the rate of adsorption are functions of the constants n and k_f. The Freundlich adsorption isotherm can be expressed [39] as,

$$\ln\ q_e = \ln k_f + \left(\frac{1}{n}\right) \ln C_e \quad (13)$$

where k_f and n are isotherm constant which indicate the capacity and intensity of the adsorption, respectively. The linear plot of $\ln q_e$ versus $\ln C_e$ at each temperature indicates that adsorption of Pb(II) also follows Freundlich isotherm. The Freundlich adsorption isotherm constants and correlation coefficients were given in Table 3. The values of k_f and n determined from the Freundlich

Table 3
Constant parameters and correlation coefficients calculated for various adsorption models at different temperatures for Pb(II) on the native (NB) and activated (AAB) bentonites.

Isotherm equation	NB			AAB		
	303 K	313 K	328 K	303 K	313 K	328 K
Langmuir						
q_0 (mg g^{-1})	19.1939	8.1103	6.4977	1.7349	2.1749	2.3175
K (L mg^{-1})	0.0038	0.0109	0.0165	0.1386	0.1429	0.1847
R^2	0.9977	0.9967	0.9930	0.9989	0.9981	0.9992
R_L	0.9811	0.9482	0.9236	0.5906	0.5833	0.5198
Freundlich						
k_f	0.8178	0.8498	0.8875	1.1372	1.2292	1.3696
n	2.6525	2.5714	2.4492	2.6954	2.2696	1.9984
R^2	0.9891	0.9960	1.0000	0.9958	0.9992	0.9941
D–R						
q_m (mol g^{-1})	0.0094	0.0084	0.0080	0.0014	0.0017	0.0024
K' (mol^2 kJ^{-2})	0.0071	0.0063	0.0055	0.0035	0.0033	0.0032
E (kJ mol^{-1})	8.3918	8.9087	9.5346	11.9523	12.3091	12.5000
R^2	0.9977	0.9962	0.9917	0.9712	0.9879	0.9997

Table 4
Thermodynamic parameters for the sorption processes Pb(II) on the native (NB) and activated (AAB) bentonites.

Adsorbent	T (K)	K	ΔG (kJ mol^{-1})	ΔH (kJ mol^{-1})	ΔS (kJ mol^{-1} K^{-1})	R^2
NB	303	0.0038	−14.0058	47.3865	0.1109	0.9904
	313	0.0109	−11.7519			
	328	0.0165	−11.1861			
AAB	303	0.1386	−4.9782	10.2961	0.0169	0.9902
	313	0.1429	−5.0630			
	328	0.1847	−4.6059			

model changed with the rise in temperature, k_f values increase with temperature. However, n values decrease with increasing temperature for Pb(II) onto NB and AAB. The value of n for Freundlich isotherm was found to be greater than 1, indicating that Pb(II) ions are favorably adsorbed by NB and AAB at all the temperature studied [40,41]. Also, a higher value of n indicates better adsorption and formation of relatively strong bond between the adsorbate and adsorbent [27].

The Dubinin–Radushkevich (D–R) adsorption isotherm model is temperature independent and a more general model than the Freundlich and Langmuir models. It predicts the energy of adsorption per unit of adsorbate and a maximum adsorption capacity for the adsorbent. The linear form of the D–R isotherm [24] is,

$$\ln\ q_e = \ln q_m - K'\varepsilon^2 \tag{14}$$

where ε (Polanyi potential) is equal to $RT\ln(1+1/C_e)$, q_e is the amount of the solute adsorbed per unit NB or AAB (mol g^{-1}), q_m the theoretical monolayer saturation capacity (mol g^{-1}), C_e the equilibrium concentration of the solute (mol L^{-1}), K' the constant of the adsorption energy (mol^2 kJ^{-2}). K' is related to mean adsorption energy (E, kJ mol^{-1}) as,

$$E = \frac{1}{(2K')^{1/2}} \tag{15}$$

The constant obtained from the plot of $\ln q_e$ versus ε^2 at 303, 313 and 328 K adsorption temperature are shown in Table 3. The difference of q_0 derived from the Langmuir and q_m from D–R models is large. The difference may be attributed to the different definition of maximum adsorption capacity in two models. In Langmuir model, q_0 represents the maximum adsorption of metal ions at monolayer coverage, whereas q_m represents the maximum adsorption of metal ions at the total specific micropore volume of the adsorbent in D–R model. The mean adsorption energy (E) gives information about chemical and physical adsorption [42]. It was found to be in the range of 8.39–12.50 kJ mol^{-1}, which is lower than the range of adsorption reaction 8–16 kJ mol^{-1}. The type of adsorption of Pb(II) onto NB and AAB was defined as physical adsorption.

3.7. Thermodynamic studies

The type of sorption may be determined through such thermodynamic quantities as Gibbs free energy (ΔG), the enthalpy change (ΔH) and entropy change (ΔS) for the sorption of Pb(II) onto NB and AAB are given in Table 4. ΔG is calculated using the following equation:

$$\Delta G = -RT\ln K \tag{16}$$

where K is the adsorption equilibrium constant (from Langmuir model). The relation between K and the thermodynamic parameters of ΔH and ΔS can be described by Van't Hoff correlation in Eq. (17):

$$\ln K = \left(\frac{\Delta S}{R}\right) - \left(\frac{\Delta H}{RT}\right) \tag{17}$$

ΔH and ΔS were calculated from the slope and intercept of Van't Hoff plots, respectively. The negative values for the Gibbs free energy change, ΔG showed that the adsorption process for the bentonite samples was feasible and spontaneous thermodynamically. However, the decrease in ΔG values with increase in temperature showed that the adsorption was not favorable at higher temperatures [43]. The positive values of ΔH indicate the endothermic behavior of the adsorption reaction of Pb(II) ions and suggest that a large amount of heat is consumed to transfer the Pb(II) ions from aqueous into the solid phase. As was suggested by Nunes and Airoldi [44], the transition metal ions must give up a larger share of their hydration water before they could enter the smaller cavities. Such a release of water from the divalent cations would result in positive values of ΔS. This mechanism of the adsorption of Pb(II) ions is also supported by the positive values of ΔS, which show that Pb(II) ions are less hydrated in the bentonite layers than in the aqueous solution. Also, the positive value of ΔS indicates the increased disorder in the system with changes in the hydration of the adsorbing Pb(II) cations. Hefne et al. [28] noted that positive ΔS value occurs as a result of redistribution of energy between the adsorbate and the adsorbent. Before adsorption occurs, the heavy metal ions near the surface of the adsorbent will be more ordered than in the subsequent adsorbed state and the ratio of free heavy metal ions to ions interacting with the adsorbent will be higher than in the adsorbed state. As a result, the distribution of rotational and translational energy among a small number of molecules will increase with increasing adsorption by producing a positive value of ΔS and randomness will increase at the solid–solution interface during the process of adsorption. The values of thermodynamic parameters for the adsorption of Pb(II) ions onto the clays are consistent with that given in the literature [39,45,46].

4. Conclusions

The adsorption efficiency increases with increasing temperature. Also, the adsorption efficiency with the AAB was greater than NB in all studied solution concentration and temperatures. The equilibrium time was 100 min. The kinetics of sorption processes were best described by a pseudo-second-order kinetic model and also fitted well the intra-particle diffusion model up to 15 min, but diffusion was not the only rate-controlling step. The activation energy of sorption was calculated using the pseudo-second-order rate constant, and it was found to be 16.51 and 13.66 kJ mol^{-1} for the NB and AAB, respectively. From the values of the activation energy, it was seen that the intra-particle diffusion kinetics was one of the rate determining steps as well as pseudo-second-order kinetics for the sorption processes. Langmuir, Freundlich and Dubinin–Redushkevich (D–R) isotherm models were used to represent the experimental data, and the models fitted well. The adsorption of Pb(II) ions onto NB and AAB was found to be endothermic according to Langmuir isotherm. R_L separation factor for Langmuir and the n value for Freundlich isotherm show that Pb(II) ions are favorably adsorbed by NB and AAB. The type of adsorption of Pb(II) ions onto NB and AAB was defined as physical adsorption. The negative value of ΔG and positive value of ΔS

showed that the adsorption of Pb(II) ions onto NB and AAB was feasible and spontaneous. The positive value of ΔH confirmed the endothermic nature of adsorption.

References

[1] N.R. Axtell, S.P.K. Sternberg, K. Claussen, Lead and nickel removal using microspora and lemna minor, Bioresour. Technol. 89 (2003) 41–48.
[2] D. Ozdes, A. Gundogdu, B. Kemer, C. Duran, Removal of Pb(II) ions from aqueous solution by a waste mud from copper mine industry: equilibrium, kinetic and thermodynamic study, J. Hazard. Mater. 166 (2–3) (2009) 1480–1487.
[3] T.G. Kazi, N. Jalbani, N. Kazi, M.K. Jamali, M.B. Arain, H.I. Afridi, A. Kandhro, Z. Pirzado, Evaluation of toxic metals in blood and urine samples of chronic renal failure patients, before and after dialyses, Renal Failure 30 (2008) 737–745.
[4] H.I Afridi, T.G. Kazi, G.H. Kazi, M.K. Jamali, G.Q. Shar, Essential trace and toxic element distribution in the scalp hair of Pakistani myocardial infarction patients and controls, Biol. Trace Elem. Res. 113 (2006) 19–34.
[5] M. Soylak, L. Elci, Y. Akkaya, M. Doğan, On-line preconcentration system for determination of lead in water and sediment samples by flow injection-flame atomic absorption spectrometry, Anal. Lett. 35 (2002) 487–499.
[6] N. Unlu, M. Ersoz, Adsorption characteristics of heavy metal ions onto a low cost biopolymeric sorbent from aqueous solution, J. Hazard. Mater. 136 (2006) 272–280.
[7] I. Chaari, E. Fakhfakh, S. Chakroun, J. Bouzid, N. Boujelben, M. Feki, F. Rocha, F. Jamoussi, Lead removal from aqueous solutions by a Tunisian smectitic clay, J. Hazard. Mater. 156 (2008) 545–551.
[8] N. Jovanovic, J. Janackovie, Pore structure and adsorption properties of an acid-activated bentonite, Appl. Clay Sci. 6 (1991) 59–67.
[9] D.C. Rodriguez-Sarmiente, J.A. Pinzon-Bello, Adsorption of sodium dodecylbenzene sulfonate on organophilic bentonites, Appl. Clay Sci. 18 (34) (2001) 173–181.
[10] O. Abollino, M. Aceto, M. Malandrino, C. Sarzanini, E. Mentasti, Adsorption of heavy metals on Na-montmorillonite, effect of pH and organic substances, Water Res. 37 (2003) 1619–1627.
[11] A.S Özcan, B. Erdem, A. Özcan, Adsorption of acid blue 193 from aqueous solutions onto Na-bentonite and DTMA-bentonite, J. Colloid Interf. Sci. 280 (2004) 44–54.
[12] R.S. Juang, S.-H. Lin, K.-H. Tsao, Mechanism of sorption of phenols from aqueous solutions onto surfactant-modified montmorillonite, J. Colloid Interf. Sci. 254 (2) (2002) 234–241.
[13] P.F. Lucham, S. Rossi, The colloidal and rheological properties of bentonite, Suspensions, Adv. Colloid Interf. Sci. 82 (1999) 43–92.
[14] J. Środoń, Nature of mixed-layer clays and mechanisms of their formation and alteration, Annu. Rev. Earth Planet. Sci. 27 (1999) 19–53.
[15] K.G. Bhattacharyya, S. Sen Gupta, Pb(II) uptake by kaolinite and montmorillonite in aqueous medium: influence of acid activation of the clays, Colloids Surf. A 277 (2006) 191–200.
[16] J.L. Venaruzzo, C. Volzone, M.L. Rueda, J. Ortiga, Modified bentonitic clay minerals as adsorbent of CO, CO_2 and SO_2 gases, Micropor. Mesopor. Mater. 56 (2002) 73–80.
[17] E. Eren, B. Afsin, Y. Onal, Removal of lead ions by acid activated and manganese oxide-coated bentonite, J. Hazard. Mater. 161 (2009) 677–685.
[18] E.P. Barrett, L.G. Joyner, P.H. Halenda, The determination of pore volume and area distributions in porous substance. I. Computations from nitrogen isotherms, J. Am. Chem. Soc. 73 (1951) 373–380.
[19] E. Eren, Removal of lead ions by Unye (Turkey) bentonite in iron and magnesium oxide-coated forms, J. Hazard. Mater. 165 (2009) 63–70.
[20] Y.S. Ho, G. Mckay, Sorption of dye from aqueous solution by peat, Chem. Eng. J. 70 (1998) 15–124.
[21] S. Lagergren, About the theory of so-called adsorption of soluble substances, Kungliga Svenska Vetenskapsakademiens, Handlingar 24 (4) (1898) 1–39.
[22] Y.S. Ho, G. Mckay, Pseudo-second order model for sorption processes, Process. Biochem. 34 (1999) 451–465.
[23] W.J. Weber Jr., Kinetics of adsorption on carbon from solution, J. Sanit. Eng. Div., ASCE 89 (SA2) (1963) 31–39.
[24] A. Sarı, M. Tuzen, D. Cıtak, M. Soylak, Adsorption characteristics of Cu(II) and Pb(II) onto expanded perlite from aqueous solution, J. Hazard. Mater. 148 (2007) 387–394.
[25] S. Tunali, T. Akar, A. Safa Özcan, I. Kiran, A. Özcan, Equilibrium and kinetics of biosorption of lead(II) from aqueous solutions by *Cephalosporium aphidicola*, Sep. Purif. Technol. 47 (2006) 105–112.
[26] Y. Liu, X. Shen, Q. Xian, H. Chen, H. Zou, S. Gao, Adsorption of copper and lead in aqueous solution onto bentonite modified by 4′-methylbenzo-15-crown-5, J. Hazard. Mater. 137 (2006) 1149–1155.
[27] J.U. Kenedy Oubagaranadin, Z.V.P. Murthy, Adsorption of divalent lead on a montmorillonite-illite type of clay, Ind. Eng. Chem. Res. 48 (2009) 10627–10636.
[28] J.A. Hefne, W.K. Mekhemer, N.M. Alandis, O.A. Aldayel, T. Alajyan, Kinetic and thermodynamic study of the adsorption of Pb(II) from aqueous solution to the natural and treated bentonite, Int. J. Phys. Sci. 3 (11) (2008) 281–288.
[29] B. Acemioğlu, Batch kinetic study of sorption of methylene blue by perlite, Chem. Eng. J. 106 (1) (2005) 73–81.
[30] T. Mathialagan, T. Viraraghavan, Adsorption of cadmium from aqueous solution by perlite, J. Hazard. Mater. B 94 (2002) 291–303.
[31] P. Antonio, K. Iha, M.E.V. Suárez-Iha, Kinetic modelling of adsorption of di-2-pyridylketone salicyloylhydrazone on silica gel, J. Colloid Interf. Sci. 307 (2007) 24–28.
[32] I.A.W. Tan, B.H. Hameed, A.L. Ahmad, Equilibrium and kinetic studies on basic dye adsorption by oil palm fibre activated carbon, Chem. Eng. J. 127 (2007) 111–119.
[33] W.L. McCabe, J.C. Smith, P. Harriott, Unit Operations of Chemical Engineering, 5th ed., McGraw-Hill, Singapore, 1993.
[34] I. Langmuir, The adsorption of gases on plane surfaces of glass, mica and platinum, J. Am. Chem. Soc. 40 (1918) 1361–1403.
[35] P.C. Mishra, R.K. Patel, Removal of lead and zinc ions from water by low cost adsorbents, J. Hazard. Mater. 168 (1) (2009) 319–325.
[36] R. Han, Z. Lu, W. Zou, W. Daotong, J. Shi, Y. Jiujun, Removal of copper(II) and lead(II) from aqueous solution by manganese oxide coated sand: II. Equilibrium study and competitive adsorption, J. Hazard. Mater. 137 (2006) 480–488.
[37] T.W. Weber, R.K. Chakravorti, Pore and solid diffusion models for fixed-bed adsorbers, AIChE 20 (1974) 228–238.
[38] C.A. Başar, Applicability of the various adsorption models of three dyes adsorption onto activated carbon prepared waste apricot, J. Hazard. Mater. B 135 (2006) 232–241.
[39] H. Freundlich, Colloid and Capillary Chemistry, Methuen, London, 1926.
[40] S.D. Faust, O.M. Aly, Adsorption Processes for Water Treatment, Butterworths, 1987.
[41] P.K. Malik, Use of activated carbons prepared from sawdust and rice-husk for adsorption of acid dyes: a case study of acid yellow 36, Dyes Pigments 56 (3) (2003) 239–249.
[42] W. Riemam, H. Walton, Ion Exchange in Analytical Chemistry, International Series of Monographs in Analytical Chemistry, 38, Pergamon Press, Oxford, 1970.
[43] A. Sarı, M. Tuzen, D. Cıtak, M. Soylak, Equilibrium, kinetic and thermodynamic studies of adsorption of Pb(II) from aqueous solution onto Turkish kaolinite clay, J. Hazard. Mater. 149 (2007) 283–291.
[44] L.M. Nunes, C. Airoldi, Some features of crystalline α-titanium hydrogenphosphate, modified sodium and n-butylammonium forms and thermodynamics of ionic exchange with K^+ and Ca^{2+}, Thermochim. Acta 328 (1999) 297–305.
[45] D Xu, X.L. Tan, C.L. Chen, X.K. Wang, Adsorption of Pb(II) from aqueous solution to MX-80 bentonite: effect of pH, ionic strength, foreign ions and temperature, Appl. Clay Sci. 41 (2008) 37–46.
[46] R. Donat, A. Akdogan, E. Erdem, H. Cetisli, Thermodynamics of Pb^{2+} and Ni^{2+} adsorption onto natural bentonite from aqueous solutions, J. Colloid Interf. Sci. 286 (2005) 43–52.